Mon. Not. R. Astron. Soc. **321**, 450–462 (2001)

Observational signatures of feedback in QSO absorption spectra

Tom Theuns,[1,2]★ H. J. Mo[2] and Joop Schaye[1]
[1]*Institute of Astronomy, Madingley Road., Cambridge CB3 0HA*
[2]*Max-Planck Institut für Astrophysik, Postfach 123, 85740 Garching, Germany*

Accepted 2000 September 12. Received 2000 August 21; in original form 2000 June 7

ABSTRACT

Models for the formation of galaxies and clusters of galaxies require strong feedback in order to explain the observed properties of these systems. We investigate whether such feedback has observational consequences for the intergalactic medium, as probed in absorption towards background quasars. A typical quasar sight-line intersects one protocluster per unit redshift, and significant feedback from forming galaxies or active galactic nuclei, heating the protocluster gas, will result in a large clearing of reduced absorption in the Lyα forest. Such a gap could be detected at redshift $\gtrsim 3$ when the mean opacity is high. Feedback from Lyman-break galaxies in protoclusters can be probed by the absorption lines produced in their winds. Strong feedback from galaxies has a major impact on the number and properties of absorption lines with column densities $N_{\rm H\,I} \sim 10^{16}\,{\rm cm}^{-2}$. This feedback can be probed with multiple sight-lines and by studying the unsaturated higher order lines of the Lyman series. Galactic winds from dwarf galaxies should break up into clouds, in order not to overproduce the number of absorption lines. These clouds can then coast to large distances.

Key words: hydrodynamics – galaxies: formation – intergalactic medium – quasars: absorption lines – cosmology: theory – large-scale structure of Universe.

1 INTRODUCTION

In cold dark matter (CDM)-dominated cosmogonies structures grow by gravitational amplification of small primordial density perturbations. High-density regions decouple from the Hubble expansion and form gravitationally bound systems with a range of masses up to a characteristic cut-off mass that increases with decreasing redshift (Press & Schechter 1974). Early on, pressure forces are unable to separate the gas from the dark matter. Galaxies form when baryons that are dragged into the dark matter potential wells are shocked to sufficiently high temperatures and densities that the gas can cool radiatively (Rees & Ostriker 1977; White & Rees 1978).

This hierarchical picture of galaxy formation predicts the formation of too many small systems and therefore conflicts with observations of the faint-end slope of the galaxy luminosity function. In order to resolve this discrepancy, feedback is assumed to suppress the formation of most small galaxies (Larson 1974; Rees & Ostriker 1977; White & Rees 1978). The required feedback could be energy input by supernovae (SNe) associated with star formation (e.g. Dekel & Silk 1986). In more massive galaxies, feedback is assumed to be able to prevent the catastrophic loss of angular momentum of forming discs, which causes discs in simulations to be much smaller than observed discs (e.g. Navarro & Steinmetz 1997; Weil, Eke & Efstathiou 1998).

On even larger scales, the hierarchical picture based solely on gas shocking and radiative cooling also seems to conflict with observations of groups and clusters of galaxies. Without some type of feedback, shocked gas in the haloes of galaxy groups will overproduce the X-ray background (Pen 1999; Wu, Fabian & Nulsen 2000). Feedback is also invoked to explain the observed deviation from self-similarity of the X-ray properties of hot gas in galaxy clusters (Kaiser 1986, 1991).

Therefore, both theoretical and observational arguments suggest that forming haloes are not just passively accreting material from the intergalactic medium (IGM), but may be a significant source of energy input into their surroundings. Is this energy injection a fairly local process, affecting only gas within a small fraction of the virial radius of the halo say, or do galaxies stir up a significant fraction of the IGM?

This question can be approached from a different angle, by studying the properties of the IGM in absorption towards background quasars. Neutral hydrogen along the line of sight produces the Lyα absorption lines observed as the quasar's 'Lyα' forest (Bahcall & Salpeter 1965; Gunn & Peterson 1965; see Rauch 1998 for a review). Several theoretical models examined whether collapsed objects could produce the observed absorption, until it was realized that the IGM itself gave rise to the majority of the lines (McGill 1990; Bi, Boerner & Chu 1991). Numerical

★ E-mail: tt@ast.cam.ac.uk

simulations of CDM-dominated cosmologies, in which the IGM is photoionized by the UV background from quasars, have been very successful in reproducing many observed properties of the Lyα forest (Cen et al. 1994; Zhang, Anninos & Norman 1995; Hernquist et al. 1996; Theuns et al. 1998b; see, e.g., Efstathiou, Schaye & Theuns 2000 for a review). For example, Theuns, Leonard & Efstathiou (1998a) showed that this model naturally reproduces the evolution in the line densities per unit redshift and unit column density, from redshift 0 to 4. The superb quality of the data that this comparison is based on increases our confidence that the current paradigm of the Lyα forest – absorption by neutral hydrogen in the intervening IGM – is basically correct.

In these simulations of the Lyα forest that do not include any feedback from forming haloes (other than the presence of a UV background), strong Lyα absorption lines (column densities $\geq 10^{15}\,\mathrm{cm}^{-2}$) are invariably produced close to forming haloes. If feedback were indeed important, as expected from the earlier theoretical arguments and from the actual observations of strong galactic winds associated with starbursts (e.g. Heckman, Armus & Miley 1990), one would expect the properties of these stronger lines to be at least partly influenced by the feedback process.

If galaxy feedback is required to explain the observed X-ray properties of groups and clusters, then real protoclusters might be very different from the protoclusters in the simulations that do not include feedback. Consequently, one might expect the absorption properties of the IGM where the line of sight intersects a protocluster to be rather different in the presence of feedback.

Metal lines (e.g., C IV) associated with $N_{\mathrm{H\,I}} \sim 10^{14.5}\,\mathrm{cm}^{-2}$ column density lines have been detected in high signal-to-noise QSO spectra (e.g. Cowie et al. 1995). Even if the lower density gas were polluted by metals at the same level, the associated C IV metal lines would generally be too weak to be detected. Ellison et al. (2000) searched for C IV in a very high-quality spectrum on a pixel-by-pixel basis, and were able to show that there must be many more metal lines than can be detected directly. Schaye et al. (2000) performed a similar search for O VI, and found evidence for oxygen enrichment down to $\tau_{\mathrm{Ly}\alpha} \sim 10^{-1}$ at $z \sim 2$–3, which corresponds to underdense gas. This is again circumstantial evidence that a galaxy can influence the gas around it out to a significant distance. The case is not so clear-cut, because the metal pollution could be the result of an earlier epoch of Population III star formation. However, if galactic winds were the source of the pollution, then these winds might change the properties of the low-density IGM as observed in absorption.

The aim of this paper is to investigate to what extent the current picture of the Lyα forest can incorporate a significant amount of feedback, without destroying the good agreement with observations. In what follows we will also use numerical simulations of the Lyα forest. We simulate a vacuum energy-dominated, flat cold dark matter model, with density parameters $(\Omega_{\mathrm{m}}, \Omega_\Lambda) = (0.3, 0.7)$ (e.g. Efstathiou et al. 1999, and references therein,), Hubble constant $h = 0.65$ (Freedman et al. 1999) and baryon density $\Omega_{\mathrm{b}}h^2 = 0.019$ (Burles & Tytler 1998) of which a fraction $Y = 0.24$ by mass is helium, normalized to the abundance of clusters (Eke, Cole & Frenk 1996). We assume the IGM to be photoionized and photoheated, and choose the spectrum of the ionizing sources such that the simulation reproduces the thermal evolution and mean absorption as determined from observations by Schaye et al. (2000b; the gas temperature as function of redshift follows the dashed line in fig. 6 of that paper). The cubic simulation box is 20 Mpc on a side (comoving), and contains 256^3 particles of each species (i.e., dark matter and gas particles; note that the designer model in Schaye et al. (2000b) was a smaller simulation but with the same thermal history), providing sufficient resolution to simulate the gas reliably (Theuns et al. 1998b). Without feedback, this simulation reproduces most of the observed properties of the Lyα forest, for this choice of currently popular values of the cosmological parameters. It includes star formation, whereby gas at a density contrast $\rho > 80\langle\rho\rangle$ is converted to 'stars', when the temperature drops below 2×10^4 K. No feedback (other than a UV background) is included.

This paper consists of two parts. In the first part (Section 2) we assume that the gas in a protocluster is pre-heated at some early time, and discuss the corresponding observational absorption signature if the line of sight to a quasar intersects the protocluster. In the second part (Section 3), we consider feedback effects from smaller systems and examine their impact on the IGM.

2 FEEDBACK ON CLUSTER SCALES

We begin this section by briefly reviewing the arguments that suggest that the entropy of protocluster gas was increased significantly by some non-gravitational process at an early time $z_{\mathrm{inj}} \geq 2$. We then argue that this gas is too hot to be confined by a galactic potential well, and hence will fill a considerable fraction of the volume of the protocluster. The probability that a quasar sight-line intersects such a hot bubble is $\sim$1 per unit redshift, and it will appear as a region of decreased absorption in the Lyα forest. This should be relatively prominent, especially at high redshift $z \geq 4$ when the mean Lyα-opacity is high. Other processes, such as proximity effects from AGN and/or galaxies in the protocluster, could contribute to clearing a gap in the absorption. Observations of metal absorption lines can be used to examine the thermal properties of the medium, and hence distinguish a protocluster gap from a void, and to make inferences about the nature of the sources producing the feedback. If the protocluster gas is in a two-phase medium, with cold clouds pressure-confined in the hot phase, then the gaps may not be completely empty.

2.1 General considerations

Clusters of galaxies are the most massive virialized systems in the Universe, with typical total masses of about $10^{15}\,\mathrm{M}_\odot$, of which 10–30 per cent is baryonic. The latter component is predominantly in the form of a hot X-ray-emitting intra cluster medium (ICM), with temperature and X-ray luminosities typically of order $T \sim 10^8$ K and $L_{\mathrm{X}} \sim 10^{45}\,\mathrm{erg\,s}^{-1}$, respectively.

The intracluster gas is believed to be shock-heated as it falls into the cluster potential well. If the initial gas temperature is negligible, then a relation $L_{\mathrm{X}} \propto T^2$ is predicted from simple scaling arguments (Kaiser 1986), which disagrees with the observed result, $L_{\mathrm{X}} \propto T^\alpha$, with $\alpha = 2.6$–3 (Jones & Forman 1984; David, Forman & Jones 1991; Lloyd-Davies, Ponman & Cannon 2000). Consequently, it was suggested that the ICM gas is 'pre-heated' by some non-gravitational process (Evrard & Henry 1991; Kaiser 1991; Navarro, Frenk & White 1995; Cavaliere, Menci & Tozzi 1997; Ponman, Cannon & Navarro 1999). The existence of such an entropy 'floor' breaks the self-similarity and helps to explain the L_{X}–T relation (Kaiser 1991). Since an initial entropy is expected to have a larger effect in clusters with lower temperature, the level of pre-heating may be revealed by measuring the specific entropy of gas in X-ray clusters as a function of cluster temperature. The effect of pre-heating would

be largest in groups of galaxies, which would emit far less X-rays when pre-heated since the hotter gas is less dense, thereby avoiding the problem of over producing the X-ray background (Wu et al. 1999b; Pen 1999).

Defining a specific 'entropy'

$$s \equiv \frac{T}{n_{\rm e}^{2/3}}, \tag{1}$$

where T is the temperature of the gas, and $n_{\rm e}$ is the electron number density, the level of pre-heating inferred from the observations is on the order of

$$s_0 \sim 100\,h^{-1/3}\,{\rm keV\,cm^2} \tag{2}$$

(Ponman, Cannon & Navarro 1999; Lloyd-Davies et al. 2000; Balogh, Babul & Patton 1999; Wu, Fabian & Nulsen 2000a). We will use $s_{100} \equiv s_0/(100\,h^{-1/3}\,{\rm keV\,cm^2})$.

At present it is not yet clear which sources dominate the heating of the ICM. The *energy* required to reach a given entropy floor increases with the gas density as $E \propto n_{\rm e}^{2/3}$, which makes it easier energetically to heat the gas before it collapses into a potential well. If supernova explosions and stellar winds, e.g., associated with episodes of rapid star formation, are the main sources of energy, then pre-heating is likely to have occurred relatively early on. Indeed, recent observations show that large numbers of stars are being formed at $z \gtrsim 3$ (Steidel et al. 1996) in strongly clustered galaxies (e.g. Adelberger et al. 1998; Giavalisco et al. 1998), which are likely progenitors of the bright galaxies in present-day clusters (Mo & Fukugita 1996; Baugh et al. 1998; Wechsler et al. 1998; Mo, Mao & White 1999). Semi-analytical models for the formation of cluster elliptical galaxies also predict that most of their stars formed at $z \gtrsim 2$ (Kauffmann, White & Guiderdoni 1993; Kauffmann et al. 1999). In addition, Mushotzky & Loewenstein (1997) argued that the observed lack of evolution in the iron abundance of cluster gas out to $z \sim 1$ also suggests that enrichment occurred early. If, on the other hand, energy input from AGN is the main energy source, then pre-heating is also likely to have occurred at $z \gtrsim 2$, because the number density of QSOs peaks around $z = 2$–3 (Shaver et al. 1996). Therefore, for both types of potential energy sources, stars or AGN, we expect that the major part of pre-heating took place before $z \sim 2$.

The inferred entropy floor (equation 2) implies that the ICM was heated to some high temperature at an early time. At a redshift z, the number density of electrons, $n_{\rm e}$, of fully ionized protocluster gas of primordial abundance (with a helium fraction of 24 per cent by mass), at overdensity δ is

$$n_{\rm e} \approx 1.2\times10^{-5}(1+\delta)\left(\frac{\Omega_{\rm b}h^2}{0.019}\right)\left(\frac{1+z}{4}\right)^3. \tag{3}$$

In order to achieve the required entropy (2), the gas in the region must be heated to a temperature

$$T \approx 0.06\left(\frac{s_{100}}{f_{\rm s}^{1/3}\phi^{2/3}}\right)(1+\delta)^{2/3} \times\left(\frac{\Omega_{\rm b}h^2}{0.019}\right)^{2/3}\times\left(\frac{1+z}{4}\right)^2\left(\frac{h}{0.65}\right)^{-1/3}{\rm keV}, \tag{4}$$

where $f_{\rm s}$ and ϕ are the heated mass and volume fractions of gas, respectively. The implied temperature is quite high ($T \gtrsim 10^6$ K; 1 keV $\approx 1.2\times10^7$ K) if pre-heating occurred at $z > 2$, even if the heating occurred close to the mean density $\delta \sim 0$. At $z < 1$, the required T is lower ($T \sim 10^5$ K) if $\delta = 0$. However, for a cluster to form at the present time, the redshift at which it turned around is about 1, in which case the gas density when the pre-heating took place must have been $\delta \sim 10$ over the volume of the protocluster, so we again obtain $T \gtrsim 10^6$ K.

If pre-heating occurred inside galaxy haloes, then $f_{\rm s}$ and ϕ are small, and the required temperature (equation 4) is higher than the virial temperature of the haloes. Such hot gas cannot be confined to a galaxy halo, and therefore, irrespective of the heat source, the pre-heated gas must have quite an extended distribution, filling a large fraction of the region occupied by a protocluster.

If pre-heating is due to SNe, one can estimate the total amount of stars needed to heat the protocluster to the required temperature. Suppose that the gas mass of the protocluster is $M_{\rm gas}$, and $f_*M_{\rm gas}$ is the mass of stars responsible for pre-heating. The total energy released by the SNe associated with those stars is

$$E = \frac{M_{\rm gas}}{\nu}f_*E_{51}10^{51}\,{\rm erg}, \tag{5}$$

where E_{51} is the energy output per SN in units of 10^{51} erg, and ν is the stellar mass needed to produce one supernova (we will write $\nu = 100\nu_{100}\,{\rm M}_\odot$). If a fraction ϵ of all of the SN energy is available to heat the gas, then the gas temperature will be

$$kT \approx 2.1\epsilon\left(\frac{E_{51}f_*}{\nu_{100}}\right){\rm keV}. \tag{6}$$

It then follows that f_* must be about $0.1\epsilon^{-1}$ to $0.2\epsilon^{-1}$ in order to heat the protocluster gas to a few million degrees. This fraction is consistent with the observed fraction of baryonic mass in stars (~10 per cent) and the metallicity of X-ray-emitting gas in clusters, if the efficiency is high, $\epsilon \sim 1$. However, if only a small part of the feedback energy goes into heating the gas, then supernova explosions and stellar winds may not be sufficient to heat the gas to the required temperature, and heating from AGN may have to be invoked (e.g. Wu et al. 2000a).

Another requirement for pre-heating to work is that the heated gas does not lose the injected entropy radiatively. The time-scale $t_{\rm cool} \equiv T/\dot{T}$ for radiative cooling is

$$t_{\rm cool} \approx 1.0\times10^{11}\sqrt{T_6}\Lambda_{-23}^{-1}\left(\frac{\Omega_{\rm b}h^2}{0.019}\right)^{-1}(1+\delta)^{-1} \times\left(\frac{1+z}{4}\right)^{-3}{\rm yr}, \tag{7}$$

where T_6 is the gas temperature in 10^6 K, and $\Lambda(T) \equiv \Lambda_{-23}\times10^{-23}\sqrt{T_6}\,{\rm erg\,cm^3\,s^{-1}}$ is the radiative cooling rate. For $T \geq 10^6$ K, cooling is dominated by thermal bremsstrahlung and $\Lambda_{-23} \sim 1$, whereas at lower temperatures $\geq 10^4$ K line-cooling becomes important and the rate can increase up to $\Lambda_{-23}(T) \sim 10^2$, depending on the metallicity and the temperature of the gas. At high temperatures and for tenuous gas, cooling will be dominated by Compton losses on the micro wave background radiation, and the cooling time $t_{\rm cool} \sim 1\times10^{10}[(1+z)/4]^{-4}$ yr. Comparing these times with the Hubble time

$$t_{\rm H} \approx 3.4\times10^9(h/0.65)^{-1}(\Omega_{\rm m}/0.3)^{-1/2}\left(\frac{1+z}{4}\right)^{-3/2}{\rm yr}, \tag{8}$$

[here and in what follows, we use the high-redshift approximation $H(z) \approx H_0\Omega_{\rm m}^{1/2}(1+z)^{3/2}$, valid for a cosmologically flat universe at $z \geq 2$] and using equation (4), we see that the cooling time is equal to the age of the Universe when $\delta \sim 100$ at $z = 3$. Again

this shows that pre-heating should occur in gas at low overdensity, since otherwise the injected entropy will be lost radiatively.

2.2 Observational signatures

In the previous section we argued that pre-heating of gas in clusters is likely to have occurred before $z \gtrsim 2$, and that the gas temperature is fairly high, $T \gtrsim 10^6$ K. We also argued that the hot gas should fill a relatively large fraction of the volume occupied by the protocluster, since the hot gas in unlikely to be confined by a galactic potential well. Because of the high temperature, the gas in a protocluster will be collisionally ionized, thereby producing a region of reduced absorption in a QSO sight-line that intersects the cluster. In addition, proximity effects due to AGN and/or galaxies may further reduce the amount of absorption. What are the expected sizes and rates of incidence of such 'gaps'?

The rate of incidence of objects with comoving density n and physical radius R is

$$\frac{\mathrm{d}N}{\mathrm{d}z} = n\pi R^2 \frac{(1+z)^2}{H(z)}. \tag{9}$$

The physical radius of a protocluster of mass $M = 10^{15} M_{15}\, h^{-1}\, \mathrm{M}_\odot$, which, at an overdensity δ at redshift z, is

$$R \approx 10 \Omega_\mathrm{m}^{-1/3} (1+\delta)^{-1/3} (1+z)^{-1} M_{15}^{1/3}\, h^{-1}\, \mathrm{Mpc}, \tag{10}$$

and consequently the average number of times a sight-line will intersect such a protocluster is (for $z \gtrsim 2$)

$$\frac{\mathrm{d}N}{\mathrm{d}z} \approx 1.9 n_4 (\Omega_\mathrm{m}/0.3)^{-7/6} (1+\delta)^{-2/3} M_{15}^{2/3} \left(\frac{1+z}{4}\right)^{-3/2}, \tag{11}$$

where n_4 is the comoving number density of protoclusters in units $4 \times 10^{-6}\, h^3\, \mathrm{Mpc}^{-3}$. For Abell clusters with mass $M_{15} \gtrsim 0.5$, $n_4 \sim 1$.

The differential Hubble velocity $V = H(z)R$ over a region of this size is

$$V = 1.6 \times 10^3 (\Omega_\mathrm{m}/0.3)^{1/6} \left(\frac{1+z}{4}\right)^{1/2} \times (1+\delta)^{-1/3} M_{15}^{1/3}\, \mathrm{km\,s^{-1}}, \tag{12}$$

and the corresponding wavelength range in a Lyα spectrum is

$$\Delta\lambda \approx 26 (\Omega_\mathrm{m}/0.3)^{1/6} \left(\frac{1+z}{4}\right)^{3/2} (1+\delta)^{-1/3} M_{15}^{1/3}\, \text{Å}. \tag{13}$$

The observational signature of a protocluster will be smaller than this, since peculiar velocities will compress the cluster's extent in redshift space. The size of the cluster given by equation (13) is large compared to the distance between lines at $z \sim 3$, and even more so at higher redshifts where the mean opacity in the forest is higher, as demonstrated in Fig. 1. This figure shows a simulated Lyα-spectrum of a $z_\mathrm{em} = 3$ and a $z_\mathrm{em} = 4$ quasar, extending over a velocity range typical for observed quasars. (Here and below, velocity v is related to wavelength λ by $\mathrm{d}v/c = \mathrm{d}\lambda/\lambda$). Such spectra do contain 'gaps' with little absorption, which are due to large voids resulting from long-wavelength perturbations, but only very rarely are such voids of the size given by equation (12), especially at the higher redshift where the mean absorption is higher. The simulation used to make Fig. 1 lacks large-scale modes due to its finite size (20 Mpc), and this may lead to an underestimate of the sizes of the largest voids. A more quantitative comparison against data could take such long-wavelength modes into account by using for example the log-normal model of Bi & Davidsen (1997).

Thus, if pre-heating of the ICM occurred at $z \gtrsim 3$, its signature may be apparent in a QSO spectrum that intersects a protocluster. Therefore, QSO absorption-line spectra are potentially powerful probes of feedback on cluster scales, since an average quasar sight-line will intersect a protocluster region of order $\sim$1 times, according to equation (11).

However, there are complications in the model prediction. At low redshifts $z \leq 1$, protoclusters may have already begun to contract relative to the Hubble flow, and the clearings in the forest produced by the hot regions in QSO spectra are smaller than when assuming pure Hubble flow. Since the line density in the Lyα forest decreases with redshift, it becomes increasingly difficult to associate a clearing in the forest with a protocluster, since such gaps naturally appear as a consequence of the emptying of voids and the overall decrease in the Lyα optical depth.

Another complication is that some cold gas may exist in the hot

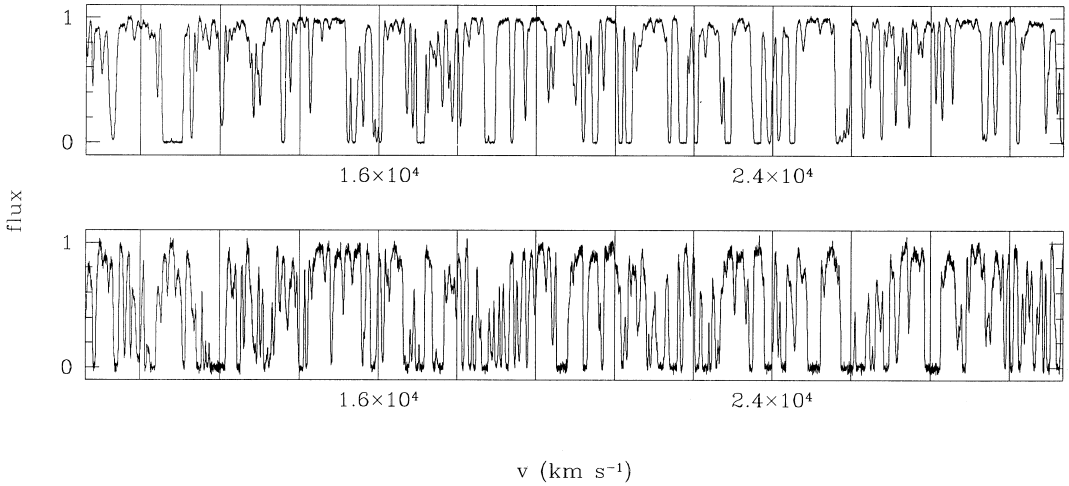

Figure 1. Simulated Lyα spectra at redshift $z = 3$ (top) and $z = 4$ (bottom), with mean absorption scaled to that of observed spectra (Schaye et al. 2000b). Vertical lines are drawn at intervals given by the expected size of a cluster, equation (12). Intervals with little absorption over a region the size of a protocluster are very rare, especially at $z = 4$ when the mean opacity is high. A spectrum of this length contains of order one protocluster, which would stand out as a region of decreased absorption if the protocluster gas were hot due to entropy injection.

protoclusters and produce Lyα absorption lines, so the clearings may not be empty. Cold gas[1] is likely to co-exist with the hot phase in the form of pressure-confined clouds, by analogy with the multiphase model of the interstellar medium (ISM) (McKee & Ostriker 1977). In these models of the ISM, cold clouds are pressure-confined by a hot medium generated by supernova explosions. Such models have also been considered for the Lyα forest itself (Ostriker & Ikeuchi 1983), as well as for the QSO absorption systems associated with galaxies (Mo 1994; Mo & Miralda-Escudé 1996).

We can estimate the properties of these cold clouds by assuming pressure equilibrium between the hot and cold phases,

$$n_{\rm c}T_{\rm c} = n_{\rm h}T_{\rm h}. \tag{14}$$

If the cold clouds are heated by the general UV background, their temperatures will be typically $\sim 10^4\,{\rm K}$. If $f_{\rm c} \equiv M_{\rm c}/M_{\rm gas}$ is the fraction of gas in the cold phase, and $m_{\rm c}$ is the typical mass of a cold cloud, then

$$C = f_{\rm c}\left[\left(\frac{n_{\rm h}}{n_{\rm c}}\right)^2 \frac{M_{\rm gas}}{m_{\rm c}}\right]^{1/3} \tag{15}$$

is the covering factor of the clouds. The mass of cold clouds in a hot medium is limited by various physical processes (evaporation, hydrodynamical and gravitational instabilities; see, e.g., Mo & Miralda-Escudé 1996), and typical values are $m_{\rm c} \sim 10^6\,{\rm M}_\odot$. Equation (15) shows that for the covering factor to be $\sim$1 requires that about 10 per cent of the protocluster gas is in the cold phase. In that case, each time we observe a clearing in the forest, produced by a protocluster, one absorption line produced by the pressure-confined clouds is expected. If this component of absorption lines is indeed important, the protocluster gap in the spectrum would be smaller.

The H I column density of a pressure-confined cloud is in the optically thin case

$$N_{\rm H\,I} \approx 1.6\times 10^{15}\,\frac{R}{1\,{\rm kpc}}\left(\frac{P}{20\,{\rm K\,cm^{-3}}}\right)^2\left(\frac{T_{\rm c}}{10^4\,{\rm K}}\right)^{-11/4} J_{21}^{-1}\,{\rm cm^{-2}}, \tag{16}$$

where P is the pressure of the confining medium, R is the cloud's radius, $T_{\rm c}$ is the temperature of the cold medium, and J_{21} is the ionization flux at the Lyman limit, in the usual units of $10^{-21}\,{\rm erg\,s^{-1}\,cm^{-2}\,sr^{-1}\,Hz^{-1}}$ (see Mo & Morris 1994). For typical values $P \sim 20$ (corresponding to $T_{\rm h} = 10^6\,{\rm K}$ and $n_{\rm h} \sim 2\times 10^{-5}\,{\rm cm^{-3}}$), the size of a cold cloud (with mass $10^6\,{\rm M}_\odot$) is about 1 kpc, and the typical H I column density of such cloud is thus $N_{\rm H\,I} \sim 10^{15.5}\,{\rm cm^{-2}}$. Therefore these pressure-confined clouds can produce strong Lyα absorption lines. Since small and diffuse clouds will evaporate in the hot environment, weak Lyα lines are not expected in the hot gap.

We will show below (Fig. 6) that the typical strong lines of column density $N_{\rm H\,I} \sim 10^{16}\,{\rm cm^{-2}}$ produced in simulations of the Lyα forest are the result of the overlap in redshift space of several filaments. The Lyα-profile of such a line is saturated, but the substructure can still be probed by the higher order lines (e.g., Lyβ). In addition, the extent of such absorbers *perpendicular* to the line of sight, which can be probed using double or lensed quasars, is very much larger than for the $\sim$1-kpc pressure-confined clouds. Therefore it is possible to distinguish strong lines produced by a single cold cloud, as described above, from those that are typical in gravitational structure formation.

If pre-heating is of stellar origin, then the ICM may be enriched in metals by supernova explosions and stellar winds. The mass-weighted mean metallicity of the protocluster gas is $Z \sim yf_*$, where y is the metal yield per unit stellar mass. Since $y \sim {\rm Z}_\odot$, we have $Z \sim f_*{\rm Z}_\odot$, i.e., the protocluster medium can be enriched to a level of 0.1–0.2 $\rm Z_\odot$, consistent with the observed metallicity of the present ICM (e.g. Renzini 1997). The absorbing clouds confined in the ICM are presumably enriched to a similar level. If this is the case, we would expect to observe strong metal lines associated with the Lyα clouds. Using the typical density and size of the cold clouds, and assuming that the UV background intensity has a power-law form $J(\nu) \propto \nu^{-1}$ with amplitude given by $J_{21} \sim 1$, the associated C IV absorption systems are expected to have column densities of 10^{13}–$10^{14}\,{\rm cm^{-2}}$, comparable to the observed C IV column densities associated with the strong lines in the Lyα forest (e.g. Cowie et al. 1995). If the hot ICM is polluted by metals as well, then a protocluster gap may be associated with very broad metal lines, due to the high gas temperature and differential Hubble expansion across the region. Such a characteristic signature may help in distinguishing a protocluster gap from a void.

If, on the other hand, heating and metal enrichment have different origins (e.g., heating was done by AGN), metals produced by supernovae and stellar winds may be confined to small regions around individual galaxies. In this case, a large fraction of the heated ICM may remain at low metallicity, and the strong Lyα lines produced by pressure-confined clouds may not be associated with any strong metal lines. Thus, by measuring the metallicities of the strong lines produced in the protocluster regions, we may hope to obtain constraints on the sources responsible for the pre-heating. Protocluster regions may be identified as large concentrations of galaxies in the galaxy distribution. Analyses of QSO absorption spectra behind such regions are therefore important.

Since the ICM is confined in the protocluster potential, the gas will move with the dark matter as the protocluster expands and collapses. We therefore do not expect to see wind-driven shells to form on the boundary of a protocluster.

2.3 Connection with Lyman-break galaxies

Large numbers of star-forming galaxies have been discovered at $z \gtrsim 3$ by colour selection using the Lyman-break technique (Steidel et al. 1996). The star formation rates in these galaxies, as inferred from their UV luminosities, are in the range 10 to $1000\,{\rm M}_\odot\,{\rm yr^{-1}}$ (for a flat universe with $\Omega_{\rm m} = 0.3$ and for a mean dust correction of $\sim$7). The strong clustering of these galaxies is consistent with many of them being the progenitors of the early-type galaxies as seen in clusters today (e.g. Mo & Fukugita 1996; Governato et al. 1998). Thus, if pre-heating of the protocluster medium occurred at $z \gtrsim 3$, we may hope to see the kind of signatures discussed in the last subsection in the spectra of QSOs which lie behind a large cluster of Lyman-break galaxies (LBGs).

There is an interesting, though indirect, argument (Pagel 1999; see also Pettini 1999) that the metals returned from LBGs are mostly in hot gas. Indeed, if all the metals ejected from LBGs were in cold gas, they should be observed as metal line systems associated with Lyα absorption systems. However, the observed total amount of metals in Lyα absorption systems is much lower than that expected from the star formation inferred to occur in LBGs. A possible solution is that most metals are hidden in hot gas which

[1] The sight-line may also intersect a galaxy. If the cluster contains 10^3 galaxies, then the covering factor of intersecting one within $30\,h^{-1}\,{\rm kpc}$ is $10^3 \times [0.03(1+z)/10]^2 \sim 0.1$ for a $R = 10\,h^{-1}\,{\rm Mpc}$ cluster at $z = 3$.

would not produce significant Lyα absorption. If this is the case, then metals are most likely contained in the protocluster medium, rather than being confined around individual galaxies, because radiative cooling would be very efficient if the gas were confined to such high-density regions (see equation 7). Alternatively, the apparent scarcity of metals could be a selection effect, when metal-rich LBGs block background quasars due to dust obscuration. Clearly, observations of the protocluster medium around LBGs can help to distinguish between these two possibilities.

If metal-enriched gas is being ejected from LBGs into the protocluster medium by winds, then we may hope to observe the signature of such gas outflows. Because of their high star formation rate, LBGs are considered to be the high-redshift counterpart of local starburst galaxies (e.g. Heckman 2000). Therefore we can use observed properties of local starbursts to predict the observable signatures of LBGs in the QSO absorption-line spectra. As summarized in Heckman et al. (2000), local starbursts are regions of intense star formation (more than $10\,\mathrm{M}_\odot$ stars are being formed per year, in a region of $\sim$1 kpc), which generally show gas outflows with velocities in the range 400–800 $\mathrm{km\,s^{-1}}$. These high outflow velocities do not depend strongly on the depth of the potential well (Heckman 2000), and are sufficiently high that a galaxy can in principle pollute a large volume of the IGM in a Hubble time. The mass outflow rate is roughly proportional to the star formation rate in the galaxy, $\dot{M}_\mathrm{w} \propto \dot{M}_*$, with the proportionality factor being typically a few. The wind consists mainly of cold clouds entrained in the outflowing hot gas. The ratio between the mass outflow rate and the rate at which mass is being returned by supernova explosions and stellar winds is typically 5 to 10. However, only about 10 per cent of the energy output from supernova explosions and stellar winds is in the kinetic energy of the cold flow; the rest is in the thermal and kinetic energy of the hot wind.

We can construct a simple model (see also Wang 1995a,b) for the properties of the winds around LBGs, assuming them to have similar outflow properties as starbursters. The density structure in a steady wind is

$$\rho_\mathrm{w}(r) = \frac{\dot{M}_\mathrm{w}}{\omega r^2 v_\mathrm{w}}, \tag{17}$$

where v_w is the wind velocity, and ω is the solid angle into which the wind blows. Inserting numerical values typical for a starburst wind gives for the hydrogen number density:

$$n_\mathrm{H}(r) \sim 1\times10^{-2}\left(\frac{\omega}{4\pi}\right)^{-1}\left(\frac{\dot{M}_\mathrm{w}}{100\,\mathrm{M}_\odot\,\mathrm{yr}^{-1}}\right) \times\left(\frac{v_\mathrm{w}}{200\,\mathrm{km\,s^{-1}}}\right)^{-1}\times\left(\frac{r}{10\,\mathrm{kpc}}\right)^{-2}\mathrm{cm}^{-3}. \tag{18}$$

In the presence of an ionizing background, the neutral fraction of gas with clumping factor $\zeta \equiv \langle n_\mathrm{H\,II}^2\rangle/\langle n_\mathrm{H\,II}\rangle^2$ is

$$\frac{n_\mathrm{H\,I}}{n_\mathrm{H}} \sim 4\times10^{-4}T_4^{-3/4}\frac{\zeta}{J_{21}}\left(\frac{n_\mathrm{H}}{10^{-3}\,\mathrm{cm}^{-3}}\right), \tag{19}$$

where $T_4 \sim 1$ is the temperature of the photoionized gas in units of 10^4 K, and the spectrum of the ionizing radiation is $\propto\nu^{-1}$ (e.g. Peebles 1993, section 23). Combining these two equations, we find for the neutral hydrogen column density at an impact parameter l

$$N_\mathrm{H\,I} \sim 1\times10^{15}T_4^{-3/4}\frac{\zeta}{J_{21}}\left(\frac{\omega}{4\pi}\right)^{-2}\left(\frac{\dot{M}_\mathrm{w}}{100\,\mathrm{M}_\odot\,\mathrm{yr}^{-1}}\right)^2 \times\left(\frac{v_\mathrm{w}}{200\,\mathrm{km\,s^{-1}}}\right)^{-2}\left(\frac{l}{50\,\mathrm{kpc}}\right)^{-3}\mathrm{cm}^{-2}. \tag{20}$$

Thus a QSO sight-line passing near a LBG will show a relatively strong, possibly broad Lyα line, associated with the wind driven by the starburst. Complex velocity structure is to be expected if the outflow is clumpy. For an impact parameter smaller than $\sim$10 kpc, the QSO sight-line goes through optically thick clouds, and a Lyman limit system or a damped Lyα system will be produced.

The observational results by Pettini et al. (2000) for the spectrum of the gravitationally lensed galaxy MS1512-cB58 (at $z = 2.73$) give direct evidence for such gas outflows with velocities $\sim$200 $\mathrm{km\,s^{-1}}$ in LBGs. However, common LBGs are too faint to yield spectra with high signal-to-noise ratios. Such outflows may be studied more efficiently is absorption towards background QSOs.

Because of their large velocities, winds from LBGs may drive shocks into the protocluster medium as they escape the potential wells of their parent haloes. In the adiabatic phase, the shock front has a density contrast of about 4 with respect to the ambient medium, and a temperature $T \sim \mu v_\mathrm{w}^2/2k \sim 2\times10^6(v_\mathrm{w}/200\,\mathrm{km\,s^{-1}})^2$ K, where μ is the mean molecular weight of the gas. Using equation (7) we see that the shocked gas will remain very hot, as it is not be able to cool within a Hubble time. Thus the winds may drive hot shells into the medium, which will eventually thermalize in the ambient protocluster gas. Since the gas in these shells is collisionally ionized, they are not expected to produce strong lines.

In summary: a typical $z \sim 3$ quasar spectrum will intersect one protocluster per unit redshift. If the gas in this cluster is hot, as is expected from models that invoke pre-heating to explain the observed X-ray properties of clusters, then a large region with little Lyα absorption would result, which might also produce associated metal absorption in the form of Hubble-broadened metal lines if the ICM is metal-enriched. Such clearings in the forest would be apparent at sufficiently high redshifts, when the mean opacity in the Lyα forest is high. Proximity effects, due to AGN and/or galaxies, might make the clearing even more distinct. However, if the protocluster gas is in a two-phase medium, with cold clouds pressure-confined in the hot medium, then these clouds may produce strong lines themselves. These could be distinguished from the more usual strong lines by the absence of substructure, probed by higher order Lyman lines, or by their small sizes, as measured from multiple quasar sight-lines. If the cold phase is metal-enriched, there would be a strong metal line associated with these lines. If protoclusters usually contain a large number of Lyman-break galaxies, then QSO spectra taken through such a concentration can be used to test these predictions. Winds from LBGs are also expected to produce strong lines with column densities $>10^{15}\,\mathrm{cm}^{-2}$ out to large impact parameters. These lines may have associated metal absorption if the wind is enriched.

3 FEEDBACK FROM SMALL SYSTEMS

Feedback on the scale of galaxy haloes appears to be required for a variety of reasons. Without feedback, a major fraction of all baryons will cool and form stars in small haloes at high redshift, exhausting the baryon supply to make up the IGM and the discs at lower redshift. This is known as the overcooling problem. The presence of an ionizing background, for example due to AGN, may suppress the collapse of baryons into dark haloes of circular speeds below $\sim$20–30 $\mathrm{km\,s^{-1}}$ (Efstathiou 1992; Quinn, Katz & Efstathiou 1996; Thoul & Weinberg 1996). For more massive

systems, feedback associated with star formation is usually invoked to explain the low baryon content of dwarf galaxies, and also to prevent forming galactic discs from losing most of their angular momentum to their dark halo (Weil et al. 1998).

The basic picture for star formation feedback is that hot bubbles blown by SNe and stellar winds overlap and power a galactic wind. Cosmic rays produced in the SNe shocks may also contribute (Breitschwerdt, McKenzie & Völk 1991). This feedback process heats cold gas, which is then no longer available for star formation, and may blow some fraction of the baryonic material out of the virial radius of the halo. In the next step of the merging hierarchy, the blown-out gas may once more be accreted.

Semi-analytical models of galaxy formation (e.g. Kaufmann et al. 1993; Lacey et al. 1993) require that a significant fraction of the total energy associated with SNe explosions be converted into thermal energy of the heated gas. However, numerical simulations of this process (e.g. Navarro & White 1994) fail to reach the required efficiency, because SN explosions invariably occur in dense gas which rapidly cools radiatively. Presently it is not yet clear whether the high efficiencies assumed in the semi-analytic models are unrealistic, or whether the simulations grossly underestimate the efficiency because they lack the resolution to produce a multiphase medium.

Efstathiou (2000) recently proposed a model where feedback produces a multi phase interstellar medium in which a low rate of star formation can produce steady conversion of cold gas into hot gas, which then drives a wind. In this model, star formation is quenched because SNe explosions limit the amount of cold gas available for star formation. The model shows that a galaxy with circular speed $\sim 50\,\mathrm{km\,s^{-1}}$ can expel 60–80 per cent of its gas over a time-scale of $\sim 1\,\mathrm{Gyr}$. Nath & Trentham (1997) also investigated a model where an early population of dwarfs underwent strong mass loss through winds, and showed that this could pollute the low-density IGM to a value close to those inferred from observations. The details of how such a wind interacts with the infalling gas may be very important for a realistic description of the feedback process, and also for estimating to what extent a forming galaxy can influence its surroundings. For example, Efstathiou (2000) argued that the wind might break up into clouds which do not interact strongly with the accreting gas. Therefore, such a galaxy would undergo inflow and outflow simultaneously.

In the next sections, we use our simulations to investigate two very simple models for possible effects of galaxy feedback on the Lyα forest. In the first model, we remove all the gas in the surroundings of galaxies so that it no longer contributes to the absorption. In this 'maximal feedback' model, we assume that galactic outflows are very powerful and heat up a significant fraction of the IGM surrounding them. We will show that this has a dramatic effect on the number of strong absorption lines. In the next section, we examine the effects of galactic winds around dwarfs on the IGM. We show that shells formed from such a wind will overproduce the number of Lyα-lines, unless the wind breaks up into clouds.

3.1 Feedback and strong lines

In the traditional picture of the Lyα forest, strong lines (column density $\geq 10^{15}\,\mathrm{cm^{-2}}$) are produced close to collapsing haloes, which typically consist of a central concentration of high-density, cooled gas which is surrounded by a hot halo of shocked gas. The hot halo itself is collisionally ionized, and consequently contributes very little to the absorption. This is illustrated in Fig. 2, where we compare a stretch of absorption spectrum with and without the contribution from hot gas. Here, gas at a given density ρ is considered 'hot' if its temperature is more than 20 per cent higher than the minimum temperature at that density. Even though this is a rather low limit, the spectrum shown in Fig. 2 is the only stretch of spectrum within a longer spectrum of length $4\times 10^4\,\mathrm{km\,s^{-1}}$ (the typical length of a $z=3$ QSO Lyα spectrum) where there is *any* noticeable contribution of the hot component. Consequently, as long as feedback on the hot component has no dynamical effects, it is unlikely to affect the observed properties of the Lyα forest.

However, if feedback also affects the cold and dense gas in the surroundings of a halo, it may have an important effect on the Lyα spectrum. We have run a standard friends-of-friends group finder (linking length 0.2 times the mean interparticle separation) on all stars in the simulation and identified 'galaxies' as groups of more than 10 'stars' (one particle has mass $1.3\times 10^6\,\mathrm{M_\odot}$, so the minimum stellar mass in a galaxy is $1.3\times 10^7\,\mathrm{M_\odot}$). We then assumed that galaxy feedback is able to heat all the gas within a physical radius R around the galaxy to such high temperatures that it no longer contributes to the absorption. We choose $R=150\,\mathrm{kpc}$ (i.e., a significant fraction of the virial radius of a large galaxy), in which case the volume filling factor, $n_{\mathrm{gal}}(4\pi/3)R^3=1$, where n_{gal} is the number density of galaxies. (The true volume filling factor of hot gas is then much lower, since these clustered haloes overlap considerably.)

Fig. 3 compares a stretch of simulated spectrum (at $z\approx 3$, panel a), with a simulated spectrum with feedback (panel b). The simulated spectra are scaled to have the same mean absorption as the spectrum of QSO 1422+231 (Rauch et al. 1997). Feedback significantly decreases the number of strong lines, since the gas that originally produced these lines is now assumed to be hot (compare, e.g., the lines at $v\approx 2000\,\mathrm{km\,s^{-1}}$ in panels a and b). Conversely, weak lines in panel (a) appear much stronger in panel (b), since the spectra are scaled to the same mean absorption. Spectrum (a), without feedback, looks similar to the observed spectrum of QSO 1422+231 in terms of the number of strong lines, whereas spectrum (b), which mimics strong feedback, has

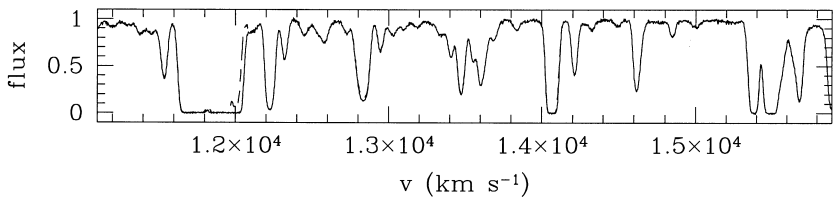

Figure 2. Simulated Lyα spectrum with (full line) and without (dashed line) the contribution from hot gas (see text for definition of 'hot'). This stretch was carefully picked to show any difference at all between these two cases: hot gas contributes very little to the observed spectrum, as expected.

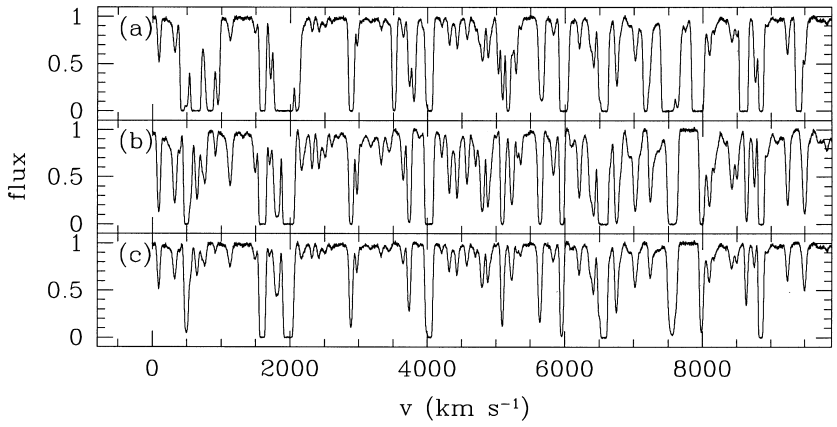

Figure 3. Simulated Lyα spectra at $z \approx 3$. Panel (a): simulated spectrum without feedback; panel (b): same as panel (a) but with feedback and scaled to have the same mean absorption as the spectrum in (a) (see text for details). Spectrum (b) contains many fewer strong lines. Panel (c) is the same as panel (b), but assuming the same amplitude of the ionizing background as in panel (a).

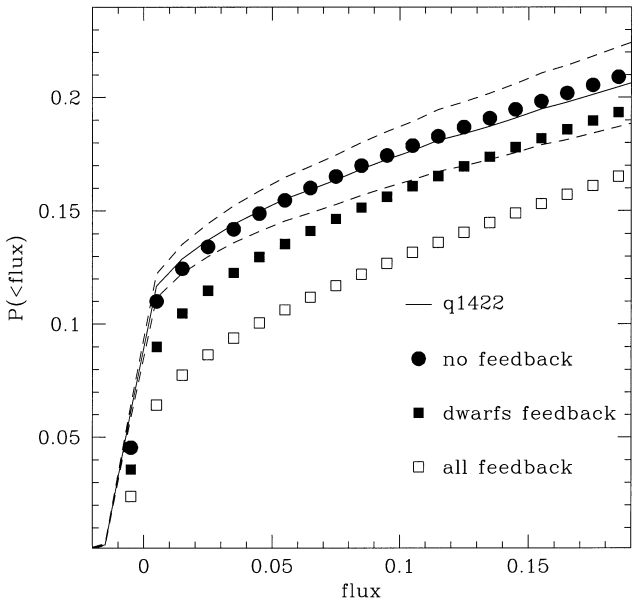

Figure 4. Comparison of the cumulative fraction of pixels with flux greater than some value. Full line: spectrum of QSO 1422, with 1σ error contours (dashed lines); filled circles: simulated spectrum without feedback; squares: simulated spectra with feedback due to dwarf galaxies (filled squares) and due to all galaxies (open squares) see text for details. Feedback has a significant effect on the number of pixels with high absorption, flux ≤ 0.2.

far fewer strong lines. Panel (c) is a spectrum with feedback, but not scaled to the same mean absorption, i.e., assuming the same amplitude for the ionizing background as in panel (a). This illustrates the effect of the rescaling.

Indeed, the removal of saturated regions due to feedback has a clear observational signature in a more detailed analysis. Fig. 4 compares the one-point functions (histogram of the flux per pixel) of the spectra shown earlier. Whereas the simulated spectrum without feedback reproduces the observed one-point function very well, the simulations that mimic feedback produce significantly fewer pixels with high absorption (flux ≤ 0.2). Two such simulations are illustrated in Fig. 4; the one labelled 'dwarfs' includes feedback from galaxies with mass $1.3 \times 10^7 \leq M/\mathrm{M}_\odot \leq 1.3 \times 10^8$, and the one labelled 'all' includes feedback from all galaxies above $1.3 \times 10^7\,\mathrm{M}_\odot$. In both cases, the radius of the sphere R around the galaxy from which the cold gas is removed, prior to computing the mock absorption spectra, equals $R = 150$ kpc, and the volume filling factors are then $\approx$0.1 and $\approx$1 for dwarfs and all galaxies, respectively. [We recall that these volume filling factors are simply the ratio of the sum of the volumes of all bubbles to the total volume. The *true* fractions of volume encompassed by the bubbles, i.e., taking into account that the bubbles overlap, are 6.5 and 30 per cent for the dwarfs and all galaxies, respectively. If we increase R to 220 kpc for the dwarfs simulation – in which case the volume filling factor increases to $\sim$1 (true volume filling factor 38 per cent) – the one-point function (as well as the number of strong lines, to be discussed next), hardly changes.] Cold gas surrounding the more massive galaxies produces a relatively large fraction of the saturated pixels, which explains the difference between imposing feedback on all galaxies, or only on the small ones.

Cen (1997) argued that the high-end of the Lyα optical depth distribution is quite sensitive to the amplitude of the power spectrum, because it probes the tail of the (e.g., Gaussian) density probability distribution. If feedback effects are strong, then the ability of this statistic to distinguish between cosmological models may be partly compromised.

The consequence of having fewer strong lines, in the presence of feedback, can also be seen when plotting the column density distribution, $\mathrm{d}^2N/\mathrm{d}N_{\mathrm{H\,I}}/\mathrm{d}V$, the fraction of lines per unit column density, per unit spectral length in $\mathrm{km\,s^{-1}}$. We have fitted Voigt profiles to both simulations and to the observed spectrum of QSO $1422+231$, using the same fitting algorithm (an automated version of VPFIT; see Carswell et al. 1987 and Webb 1987). Fig. 5 shows that the simulation without feedback reproduces the observed numbers of strong lines very well, whereas the simulations that mimic feedback significantly underproduce the number of strong lines. Note that the shape of the column-density distribution is sensitive to the amount of large-scale power (e.g. Gnedin 1998). This could be used to distinguish the effects of feedback from those of large-scale power on the column-density distribution.

The above considerations show that this type of maximal feedback, occurring in a spherical region around the forming halo can be ruled out. However, the distribution of gas that gives rise to absorption lines is actually far from spherical. In Fig. 6 we plot the

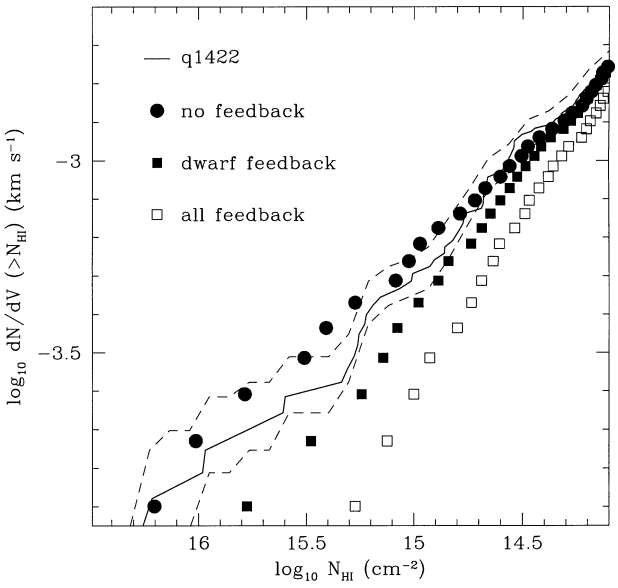

Figure 5. Cumulative number of Voigt-profile lines per unit velocity ($\mathrm{km\,s^{-1}}$), with column density larger than some value. Symbols are the same as in Fig. 4. The simulations that mimic feedback (open and filled squares) produce significantly fewer lines than the simulation without feedback (filled circles). The latter reproduces the observations (full line) very well. Dashed lines indicate the 25 and 75 percentiles for the observations, determined using bootstrap resampling.

matter distribution of a system that produces a strong line with column density $1.4\times10^{16}\,\mathrm{cm^{-2}}$. This line is a superposition of the absorption from three to four different filaments, which blend together in redshift space due to peculiar velocity gradients. The distribution of the cold gas which is responsible for the line is filamentary. Presumably, a galactic outflow from the stars near the dense knot at $v_z\sim600\,\mathrm{km\,s^{-1}}$, which contributes most to the absorption, would preferentially occur perpendicular to the filament along the path of least resistance, in which case the line may not suffer strongly from feedback after all. However, the consequence of directing all the feedback momentum into the low-density surroundings is that the accretion rate on to the halo, which is dominated by infall along the filament, cannot be strongly affected by the feedback. That is, if feedback is able to limit the accretion rate on to dwarf haloes, then it will necessarily also influence the properties of strong Lyα absorption lines. Note that the individual components that give rise to the strong line can be recognized in the higher order Lyβ line, if it is not saturated. Therefore higher order Lyman lines should be good probes of the state of the cold gas in the surroundings of forming haloes, and can be used to examine whether feedback is able to stir the accreting gas significantly.

Clearly, a more detailed analysis, for example based on probing substructure in strong lines using higher order transitions, is required, but it does seem safe to conclude that the properties of strong lines may be a valuable probe of feedback around forming galaxies. A detailed comparison of simulations without feedback with high-resolution observations may shed light on whether

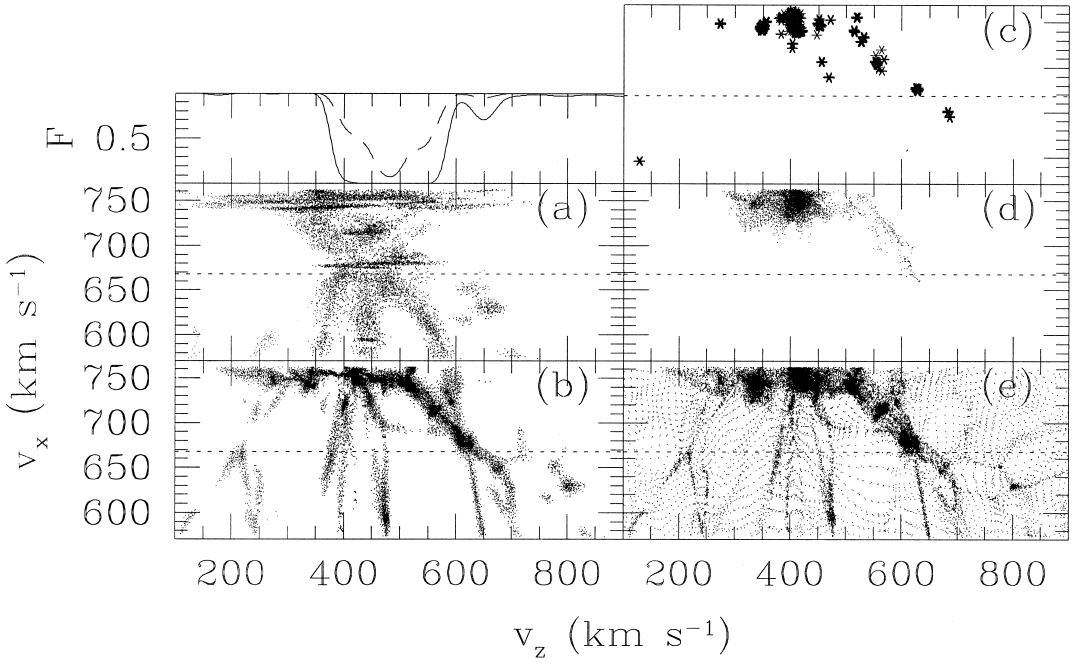

Figure 6. Geometry of the structure that produces a strong Lyα line. Top left panel: Lyα absorption spectrum (flux versus velocity) of a line with column density $1.4\times10^{16}\,\mathrm{cm^{-2}}$ (full line) and the corresponding Lyβ profile (dashed). Panels (a), (b) and (d) show the gas distribution in a thin slice along the sight-line (the dashed horizontal line in panels a–e) that produces this strong line. Plotted are gas particles with $\rho\geq\langle\rho\rangle$ and temperature $T\leq2.5\times10^4$ K (panels a–b) and hot gas particles with $T\geq2.5\times10^4$ K (panel d). Positions are labelled in Hubble velocity $v=H(z)r$. The slice in the y-direction (perpendicular to the page) is $10\,\mathrm{km\,s^{-1}}$ ($20\,\mathrm{km\,s^{-1}}$ for panel d). Star particles are plotted as stars in panel (c). In panel (a), v_z refers to the redshift space velocity, $Hr+v_{\rm pec}$. Panel (e) plots the corresponding dark matter particles. The absorption line is a superposition of three to four filaments which overlap in redshift space due to the high peculiar velocities induced by the nearby large mass concentration. These high velocities make it difficult to identify the structure in redshift space (panel a) with the corresponding filaments in real space (panel b). The massive system at the top is embedded in hot, shocked gas, but there is very little hot gas associated with the filaments that produce the line. Note that the gas density is an interpolation over the plotted SPH particles, so that particles not directly hit by the plotted line of sight may still contribute to the absorption.

galaxy feedback is an important factor in determining the properties of strong lines.

3.2 Winds from dwarf galaxies

In the previous section we discussed the effects of feedback on the immediate surroundings of the galaxy. We showed that feedback cannot influence all the cold gas around forming haloes out to ~150 kpc without significantly affecting the properties of strong lines as well. Here we discuss in more detail whether outflows from dwarf galaxies may themselves be responsible for producing absorption lines.

The mass-to-light ratio in dwarf galaxies is typically of the order $M/L \sim 100\,\mathrm{M}_\odot/\mathrm{L}_\odot$ (e.g. Carignan & Freeman 1988; Lake, Schommer & van Gorkom 1990), much higher than in spirals or ellipticals. Presumably, a wind associated with feedback from star formation was able to blow most of the gas out of the shallow potential well of the galaxy. Indeed, in the model of Efstathiou (2000), a galactic wind is able to remove 60–80 per cent of the gas contained in a dwarf galaxy, over a time-scale of order 1 Gyr. In these models, the outflow velocity at the virial radius is typically of order a few times the escape velocity, which in turn is typically a few times the circular speed ($v_{\rm circ}$) of the halo. In this case, the wind may evacuate a cavity in the IGM, surrounded by a shell.

The momentum conservation equation for a spherical shell with mass M_s and velocity V_s, which is being blown into the surrounding IGM by a galactic wind with mass-loss rate $\dot{M}_{\rm w}$ and velocity $V_{\rm w}$ is

$$\frac{\mathrm{d}}{\mathrm{d}t}(M_s V_s) = \dot{M}_{\rm w} V_{\rm w}\left(1-\frac{V_s}{V_{\rm w}}\right) - 4\pi R_s^2 \rho[C^2/\gamma + V(V_s+V)] - \frac{GM_{\rm g}M_s}{R_s^2}, \quad (21)$$

where R_s is the current position of the shell. The first term is the momentum accreted from the wind. The second term is the deceleration of the shell due to the pressure of the surrounding IGM [density $\rho(R_s)$, sound speed C, and adiabatic index γ], and due to the sweeping-up of matter which rains on to the expanding shell with velocity V. Finally, the last term is the gravitational deceleration due to the mass $M_{\rm g}$ interior to the shell (G denotes Newton's constant of gravity). The mass accretion rate of the shell due to accretion from the wind and the sweeping-up of the IGM is

$$\frac{\mathrm{d}}{\mathrm{d}t}M_s = \dot{M}_{\rm w}\left(1-\frac{V_s}{V_{\rm w}}\right) + 4\pi R_s^2 \rho(V_s+V). \quad (22)$$

The initial conditions can be set at the virial radius R_{200} of the halo, defined as usual as the radius within which the mean overdensity is 200 times the critical density. Mo, Mao & White (1998) give the relation between the virial radius, the enclosed mass M_{200}, the circular velocity $V_{\rm circ}$ and the Hubble constant at redshift z as

$$R_{200} = \frac{V_{\rm circ}}{10H(z)}, \quad (23)$$

$$M_{200} = \frac{V_{\rm circ}^3}{10GH(z)}. \quad (24)$$

We will assume $V_s = V_{\rm w}$ at $R_s = R_{200}$, and denote the fraction of (baryonic) mass swept-up by the wind by the time it reaches the virial radius by $\alpha \leq 1$. We also assume the wind-speed to be constant. Finally, we need to specify the density profile of the material surrounding the galaxy, for which we assume

$$\rho(R) = \left[\frac{200}{3}\left(\frac{R_{200}}{R}\right)^2 + 1\right]\rho_{\rm c}, \quad (25)$$

where $\rho_{\rm c} = 3H^2/8\pi G$ is the critical density. The gas density is $\Omega_{\rm b}/\Omega_{\rm m}\rho$. These equations are valid at high redshift where $\langle\rho\rangle \approx \rho_{\rm c}$.

Equations (21) and (22) can be cast in dimensionless form, using R_{200}, $V_{\rm w}$ and M_{200} as the units of distance, velocity and mass, respectively. Using lower-case letters to denote dimensionless variables, we find

$$\frac{\mathrm{d}}{\mathrm{d}\tau}(m_s v_s) = \frac{\dot{M}_{\rm w} t_*}{M_{200}}(1-v_s) - \Omega_{\rm b} r_s^2 (r_s^{-2} + 3/200) \times [(v+v_s)v + c^2/\gamma] - v_{\rm circ}^2(1+\chi-m_s)m_s/r_s^2, \quad (26)$$

$$\frac{\mathrm{d}}{\mathrm{d}\tau}m_s = \frac{\dot{M}_{\rm w} t_*}{M_{200}}(1-v_s) + \Omega_{\rm b} r_s^2 (r_s^{-2} + 3/200)(v+v_s), \quad (27)$$

where $\chi \equiv (r_s - 1) + (r_s^3 - 1)/200$, and the time variable $\tau = t/t_*$ with $t_* = R_{200}/V_{\rm w}$.

Fig. 7 illustrates the dynamics of a wind emanating from a small galaxy with circular velocity $50\,\mathrm{km\,s^{-1}}$. We assumed that feedback is very efficient, and that the initial shell mass $M_s = \alpha(\Omega_{\rm b}/\Omega_{\rm m})M_{200}$

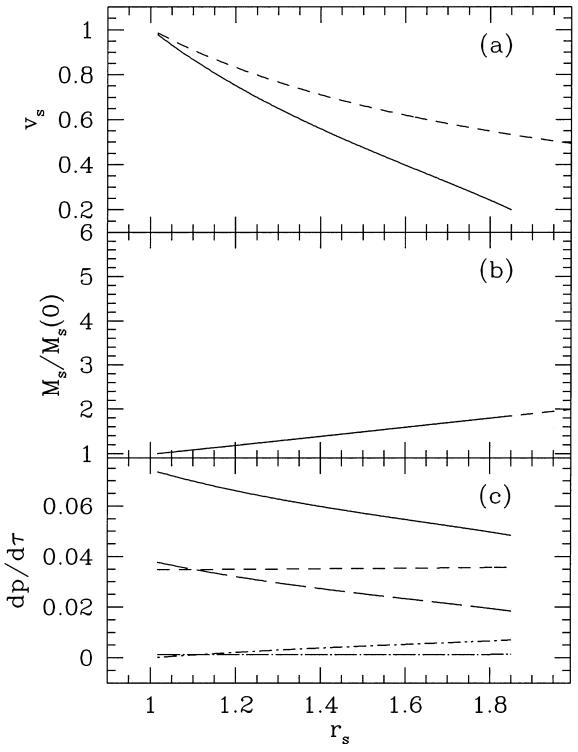

Figure 7. Dynamics of a wind with mass-loss rate $\dot{M}_{\rm w} = 0.5\,\mathrm{M}_\odot\mathrm{yr}^{-1}$ and wind-speed $100\,\mathrm{km\,s^{-1}}$, emanating from a galaxy with circular velocity $50\,\mathrm{km\,s^{-1}}$ into the IGM with sound speed $20\,\mathrm{km\,s^{-1}}$ at a redshift $z = 3$. (We assumed in addition $h = 0.65$, $\Omega_{\rm b} = 0.05$ and $\Omega_{\rm m} = 0.3$ for the cosmological parameters.) Panel (a) depicts the velocity of the shell (in units of the wind velocity) versus its position (in units of the virial radius $R_{200} = 17.5$ kpc of the halo). Panel (b) shows the mass of the shell, in units of the initial mass. The dashed curves neglect the forces acting on the shell. Panel (c) shows the magnitude of the dimensionless forces acting on the shell. From top to bottom, the curves denote the total force (full line), gravity (short dashed), ram-pressure force of the surrounding IGM (long-dashed), ram-pressure of the wind (dot-short-dashed), and the thermal pressure of the IGM (short-dashed–long-dashed.

with $\alpha = 1$. We further assumed that gas is accreting on to the galaxy with velocity $V = V_{\rm circ}$, and integrated the equations until the stagnation point where the velocity becomes sonic, $V_s = C$. The deceleration of the shell is dominated by gravity (mostly from the halo) in this case, with a non-negligible contribution from the ram-pressure of the infalling gas. Nath & Trentham (1997) followed Tegmark, Silk & Evrard (1993) and neglected the gravity of the halo, as did Ferrara, Pettini & Shchekinov (2000) when they estimated the distance to which a wind-blown shell will travel and pollute the IGM. In our case, the shell travels out to $\sim$1.8 times the viral radius, thereby doubling its mass. The dashed lines in panels (a) and (b) illustrate the case where forces are neglected, in which case the shell reaches a considerably larger distance, sweeping up $\sim V_{\rm w}/C$ times its initial mass.

Fig. 8 illustrates the stagnation point of the shell for different wind velocities, as a function of the circular velocity of the halo. We have assumed that a wind with mass-loss rate $\dot{M}_{\rm w} = 0.5\,{\rm M}_\odot\,{\rm yr}^{-1}$ blows for 0.5 Gyr (so that it can in principle remove a substantial fractrion of the baryons over a long time; see also Efstathiou 2000), and plot the position of the shell when it stagnates, $V_s = C$, or until $t = 1.0$ Gyr. In small haloes, winds of 100–150 km s^{-1} are able to expel gas up to 3–6 times the virial radius, but the increased gravity in more massive haloes prevents the shell from travelling far. On the other hand, if the wind velocity is a given fraction of the circular speed, then slow winds blow further in more massive haloes, since such winds can blow for longer before the shell speed becomes equal to the sound speed of the IGM.

The virial radius R_{200} of a halo is related to its circular velocity by (equations. 23 and 24)

$$R_{200} = 17\,{\rm kpc}\,\frac{V_{\rm circ}}{50\,{\rm km\,s^{-1}}}\left(\frac{\Omega_{\rm m}}{0.3}\right)^{-1/2}\left(\frac{1+z}{4}\right)^{-3/2}, \qquad (28)$$

and the corresponding virial mass

$$M_{200} = 1\times10^{10}\left(\frac{V_{\rm circ}}{50\,{\rm km\,s^{-1}}}\right)^{3}\left(\frac{\Omega_{\rm m}}{0.3}\right)^{-1/2} \times\left(\frac{h}{0.65}\right)^{-1}\left(\frac{1+z}{4}\right)^{-3/2}{\rm M}_\odot. \qquad (29)$$

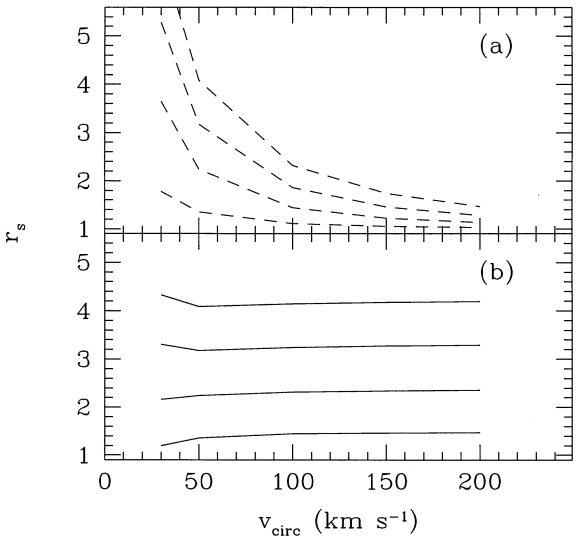

Figure 8. Stagnation radius of the shell (in units of the virial radius R_{200} of the halo) versus circular velocity of the halo, for wind velocities of 50, 100, 150 and 200 km s^{-1} (panel a), and 1, 2, 3, $4\times V_{\rm circ}$ (panel b).

Therefore for the wind parameters in Fig. 7 the final shell radius $R_s \sim 30$ kpc and the mass in the shell $M_s \sim 3.3\times10^9\,{\rm M}_\odot$, where we assumed that $\Omega_{\rm b}/\Omega_{\rm m} = 0.05/0.3 = 0.17$.

The cross-section of shells of such a size is quite high, with a mean number of intersections per unit redshift of

$$\frac{{\rm d}N}{{\rm d}z} \approx 50\,\frac{n_0}{0.5(h^{-1}\,{\rm Mpc})^3} \times\left(\frac{R_s}{30\,{\rm kpc}}\right)^2\left(\frac{h}{0.65}\right)^{-1}\times\left(\frac{\Omega_{\rm m}}{0.3}\right)^{-1/2}\left(\frac{1+z}{4}\right)^{1/2}, \qquad (30)$$

where $n_0 \sim 0.5(h^{-1}\,{\rm Mpc})^{-3}$ is the comoving number density of dwarfs (as determined from our galaxy-cluster normalized simulation). If such a shell produces absorption lines, then a significant fraction of all Lyα lines could be due to such shells. (A $z = 3$ quasar spectrum contains typically of order 300 lines above a column density of $10^{13}\,{\rm cm}^{-2}$ per unit redshift).

Note that one would expect such wind blown bubbles to produce *two* lines, when punctured by a sight-line, separated by $\sim$100 km s^{-1}. Cristiani et al. (1997) analysed Lyα lines of several high-resolution quasar spectra, and concluded that the two-point correlation function of the lines shows clustering at such scales. In contrast, Pettini et al. (1990) and Stengler-Larrea & Webb (1993) claimed a non-detection of such a signal. Part of the confusion might be caused by the non-uniqueness of Voigt-profile fits, especially in the presence of severe line-blending occurring at high redshifts. A uniform comparison of high-resolution spectra with simulations is required to check for the reality of such a signal.

Below we will estimate the column density of such a shell, but first we would like to point out that there are significant uncertainties in the estimate of the shell's radius. Dwarf galaxies in simulations are invariably embedded in filaments at over-densities of a few, which have significant non-spherical infall velocities which will oppose outflows. Therefore a more realistic description of the shell's motion should take into account such a filamentary matter distribution.

More importantly, it is not clear how efficiently the outflowing gas will couple to the surrounding IGM. The wind may break up into clouds, which coast to large distances without sweeping up a significant fraction of the ambient IGM. In that case, although some of the outflowing gas may still reach large distances, the swept-up mass may be much less than that estimated above. If we assume that only a fraction f of the surrounding IGM is swept up, with the rest in cold clouds, then the total column density of the remaining gas

$$N_{\rm H} \sim 3.5\times10^{19} f\,\frac{M_s}{3\times10^9\,{\rm M}_\odot}\left(\frac{R_s}{30\,{\rm kpc}}\right)^{-2}. \qquad (31)$$

Since the wind velocity ($\sim$100 km s^{-1}) is much larger than the sound speed of the IGM, the wind results in a strong shock as it runs into its surroundings. In the adiabatic phase, the density of the shocked shell is then about 4 times that of the ambient medium (n_1), while the temperature is about $T_2 \sim 5\times10^5(v_{\rm w}/200\,{\rm km\,s^{-1}})^2$ K. Gas of such temperature and density, and with a metallicity $Z > 0.01\,{\rm Z}_\odot$, has a cooling time shorter than its age (see equation 7); at these temperatures, cooling will be dominated by metals, hence $\Lambda_{23} \gg 1$.). Thus, as the shock propagates into the medium and sweeps up gas, it can cool down to $\sim10^4$ K and become dense, with a density $n_3 \sim \mathcal{M}_1^2 n_1 \sim 100 n_1$ ($\sim10^{-3}\,{\rm cm}^{-3}$ at $z \sim 3$), where $\mathcal{M}_1$ is the initial Mach

number of the shock. Under these assumptions, the column density of the shell is

$$N_{\rm H\,I} \sim 1.4\times10^{16} f \left(\frac{T_4^{-3/4}\zeta}{J_{21}}\right)\left(\frac{n_3}{10^{-3}\,{\rm cm}^{-3}}\right)\times\frac{N_{\rm H}}{3.5\times10^{19}\,{\rm cm}^{-2}}, \quad (32)$$

where we used equation (19) for converting the total to the neutral column density.

The physical parameters for the winds from a dwarf versus those from a LBG, discussed in Section 2.3, are quite different. For the assumed mass-loss rates (0.5 for the dwarf versus $100\,{\rm M}_\odot\,{\rm yr}^{-1}$ for the LBG) and wind velocities (100 versus $200\,{\rm km\,s}^{-1}$) for these systems, the wind densities differ by a factor 1/100. Consequently, for the LBG, it is the dense, cold wind that produces most of the absorption, since the swept-up hot shell cannot cool. The reverse is true for the wind from the dwarf galaxy, for which the tenuous wind produces no significant absorption, but the dense swept-up shell produces lines.

If the wind interacts strongly with the IGM, $f \sim 1$, the high column density of the lines given by equation (32) combined with the rate of incidence of the shells, ${\rm d}N/{\rm d}z \sim 50$, predicts of order 100 lines with columns larger than $10^{16}\,{\rm cm}^{-2}$ per quasar spectrum, which is already much more than the typical total number ~20 of such lines in an observed spectrum. Therefore these considerations require $f \ll 1$, i.e., the wind cannot retain its integrity but must break up into clouds. These clouds, which may have higher column densities, are then not subject to the momentum conservation equation (21) and can coast to large distances $r \sim 0.3\,{\rm Mpc}$ if they move at $100\,{\rm km\,s}^{-1}$ over the Hubble time, (equation 8). Since these clouds are polluted by metals of the SNe explosions that drive them out of the galaxy in the first place, such winds should be able to deposit heavy elements throughout the IGM. Clearly, a much more detailed model is required to compute the covering factor of such clouds. Alternatively, the matter density in the surroundings of the halo may limit the expansion of the shell much more than we have computed here – for example, because the infall velocities are higher than we have assumed, or because the distribution is non-spherical and the winds are funnelled into the low-density surroundings without sweeping up much matter.

Finally, we would like to make a remark on the effects of such winds on neighbouring haloes. In numerical simulations of hierarchical clustering, each dark matter halo always contains a swarm of smaller haloes down to the resolution scale (e.g. Moore et al. 1999). A galactic wind would presumably remove most of the gas from such subclumps, leaving these substructures mostly dark.

In summary: strong Lyα lines may be excellent probes of feedback effects on galactic scales. If galactic feedback is assumed to heat a large fraction of the cold gas in the surroundings of forming haloes, then many fewer strong lines are produced than are observed in QSO spectra. Shells formed from gas swept up by galactic winds from dwarf galaxies would overproduce the number of strong absorption lines. Therefore we argued that these winds should break up into clouds, which can then coast to large distances and pollute the IGM with metals, or be funnelled into the low-density surroundings without producing a strong line.

4 SUMMARY

The paradigm in which the Lyα forest is produced by the low-density photoionized IGM, which traces the structure of the underlying dark matter perturbations, has been very successful in explaining properties of observed high-resolution quasar spectra. However, models of galaxy and galaxy cluster formation require large amounts of feedback in order to match the observations. We have investigated possible observational signatures of this type of feedback in Lyα spectra.

Pre-heating is often invoked to explain the observed X-ray properties of galaxy clusters. A QSO sight-line intersects of order one such protocluster per unit redshift. If the intracluster gas is hot, it will produce a large gap with little absorption in the spectrum, which could be detected at high redshift, $z \sim 3$–4, when the Lyα forest opacity is high. If the protocluster gas is in a two-phase medium, the gas in pressure-confined cold clouds could produce a single strong line with associated metals. Such a model can be tested observationally, by probing the substructure of such absorbers using, e.g., higher order Lyman lines, or by using multiple sight-lines. Dense groups of Lyman-break galaxies at $z \sim 3$–4 are likely sites of protoclusters, and QSO spectra taken through such a structure could be used to put limits on cluster pre-heating. Winds associated with star formation in Lyman-break galaxies will also produce lines with column densities $>10^{15}\,{\rm cm}^{-2}$, plausibly associated with metals escaping from the galaxy. Such lines can be used to study the feedback process in these galaxies.

Feedback on galactic scale will influence the properties of strong $N_{\rm H\,I} \sim 10^{16}\,{\rm cm}^{-2}$ Lyα lines, since these are produced close to forming haloes. If feedback is able to heat a significant fraction of the cold gas in the surroundings of a galaxy, then far fewer strong lines will be produced. However, the outflows may be preferentially directed into the low-density surroundings, in which case strong lines may survive. Shells associated with winds from dwarf galaxies will overproduce the number of absorption lines, unless the wind breaks up into clouds. These clouds can coast to large distances and pollute the IGM with metals. Alternatively, the matter surrounding the galaxy may funnel the wind into the low-density IGM, without producing strong lines.

These simple arguments suggest that feedback may have an observable effect on the Lyα forest. Some of our predictions on cluster feedback can be tested by correlating Lyα-absorption spectra with the Lyman-break galaxies along the line of sight. Simulations of dwarf galaxy formation that include a wind can be used to examine the interaction of a galactic wind with accreting gas.

ACKNOWLEDGMENTS

We thank M. Rauch and W. Sargent for providing us with the spectrum of QSO 1422+231, and G. Efstathiou for many discussions and suggestions. TT acknowledges partial funding from PPARC, and JS thanks the Isaac Newton trust and PPARC for the award of a studentship. This work has been supported by the 'Formation and Evolution of Galaxies' network set up by the European Commission under contract ERB FMRX-CT96086 of its TMR programme. The research was conducted in cooperation with Silicon Graphics/Cray Research, utilizing the Origin 2000 supercomputer at the Department for Applied Mathematics and Theoretical Physics (DAMTP), Cambridge.

REFERENCES

Adelberger K. L., Steidel C. C., Giavalisco M., Dickinson M., Pettini M., Kellogg M., 1998, ApJ, 505, 18

Bahcall J. N., Salpeter E. E., 1965, ApJ, 142, 1677
Balogh M. L., Babul A., Patton D. R., 1999, MNRAS, 307, 463
Baugh C. M., Cole S., Frenk C. S., Lacey C. G., 1998, ApJ, 498, 504
Bi H., Davidsen A. F., 1997, ApJ, 479, 523
Bi H. G., Boerner G., Chu Y., 1991, A&A, 247, 276
Breitschwerdt D., McKenzie J. F., Völk H. J., 1991, A&A, 245, 79
Burles S., Tytler D., 1998, ApJ, 499, 699
Carignan C., Freeman K. C., 1988, ApJ, 332, L33
Carswell R. F., Webb J. K., Baldwin J. A., Atwood B., 1987, ApJ, 319, 709
Cavaliere A., Menci N., Tozzi P., 1997, ApJ, 484, 21
Cen R., 1997, ApJ, 479, L85
Cen R., Miralda-Escudé J., Ostriker J. P., Rauch M., 1994, ApJ, 437, L9
Cowie L. L., Songaila A., Kim T.-S., Hu E. M., 1995, AJ, 109, 1522
Cristiani S., D'Odorico S., D'Odorico V., Fontana A., Giallongo E., Savaglio S., 1997, MNRAS, 285, 209
David L. P., Forman W., Jones C., 1991, ApJ, 380, 39
Dekel A., Silk J., 1986, ApJ, 303, 39
Efstathiou G., 1992, MNRAS, 256, 43P
Efstathiou G., 2000, MNRAS, 317, 697
Efstathiou G., Bridle S. L., Lasenby A. N., Hobson M. P., Ellis R. S., 1999, MNRAS, 303, 47
Efstathiou G., Schaye J., Theuns T., 2000, Phil. Trans. R. Soc. Lond. A, 358, 2049
Eke V. R., Cole S., Frenk C. S., 1996, MNRAS, 282, 263
Ellison S. L., Songaila A., Schaye J., Pettini M., 2000, AJ, 120, 1175
Evrard A. E., Henry J. P., 1991, ApJ, 383, 95
Ferrara A., Pettini M., Shchekinov Y., 2000, MNRAS, 319, 539
Freedman J. B., Mould J. R., Kennicutt R. C., Madore B. F., 1999, in Sato K., eds, Proc. IAU Symp. 183, Cosmological Parameters and the Evolution of the Universe. Kluwer, Dordrecht
Giavalisco M., Steidel C. C., Adelberger K. L., Disckinson M. E., Pettini M., Kellogg M., 1998, ApJ, 503, 543
Gnedin N., 1998, MNRAS, 299, 392
Governato F., Baugh C. M., Frenk C. S., Cole S., Lacey C. G., Quinn T., Stadel J., 1998, Nat, 392, 359
Gunn J. E., Peterson B. A., 1965, ApJ, 142, 1633
Heckman T., 2000, Phil. Trans. R. Soc. Lond. A, preprint (astro-ph/9912029)
Heckman T. M., Armus L., Miley G. K., 1990, ApJS, 74, 833
Heckman T. M., Lehnert M. D., Strickland D. K., Armus L., 2000, ApJS, 129, 493
Hernquist L., Katz N., Weinberg D. H., Miralda-Escudé J., 1996, ApJ, 457, L51
Jones C., Forman W., 1984, ApJ, 276, 38
Kaiser N., 1986, MNRAS, 219, 785
Kaiser N., 1991, ApJ, 383, 104
Kauffmann G., White S. D. M., Guiderdoni B., 1993, MNRAS, 263, 201
Kauffmann G., Colberg J. M., Diaferio A., White S. D. M., 1999, MNRAS, 307, 529
Lacey C. G., Guiderdoni B., Rocca-Volmerange B., Silk J., 1993, ApJ, 401, 15
Lake G., Schommer R. A., van Gorkom J. H., 1990, AJ, 99, 547
Larson R. B., 1974, MNRAS, 169, 229
Lloyd-Davies E. J., Ponman T. J., Cannon D. B., 2000, MNRAS, 315, 689
McGill C., 1990, MNRAS, 242, 544
McKee C. F., Ostriker J. P., 1977, ApJ, 218, 148
Mo H. J., 1994, MNRAS, 269, L49
Mo H. J., Fukugita M., 1996, ApJ, 467, L9
Mo H. J., Miralda-Escudé J., 1996, ApJ, 469, 589
Mo H. J., Morris S. L., 1994, MNRAS, 269, 52
Mo H. J., Mao S., White S. D. M., 1998, MNRAS, 295, 319
Mo H. J., Mao S., White S. D. M., 1999, MNRAS, 304, 175
Moore B., Ghigna S., Governato F., Lake G., Quinn T., Stadel J., Tozzi P., 1999, ApJ, 524, L19
Mushotzky R. F., Loewenstein M., 1997, ApJ, 481, L63
Nath B. B., Trentham N., 1997, MNRAS, 291, 505
Navarro J. F., Steinmetz M., 1997, ApJ, 478, 13
Navarro J. F., White S. D. M., 1994, MNRAS, 267, 401
Navarro J. F., Frenk C. S., White S. D. M., 1995, MNRAS, 275, 720
Ostriker J. P., Ikeuchi S., 1983, ApJ, 268, L63
Pagel B. E. J., 1999, in Hippelein H., ed., Galaxies in the Young Universe II. Springer-Verlag (astro-ph/9911204)
Peebles P. J. E., 1993, Principles of Physical Cosmology. Princeton Univ. Press, Princeton
Pen U-L., 1999, ApJ, 510, L1
Pettini M., 1999, in Welsh J., Rosa M., eds, Chemical Evolution from Zero to High Redshift. Springer, Berlin, p. 233
Pettini M., Hunstead R. W., Smith L. J., Mar D. P., 1990, MNRAS, 246, 545
Pettini M., Steidel C. C., Adelberger K. L., Dickinson D., Giavalisco M., 2000, ApJ, 528, 96
Ponman T. J., Cannon D. B., Navarro J. F., 1999, Nat, 397, 135
Press W. H., Schechter P., 1974, ApJ, 187, 425
Quinn T., Katz N., Efstathiou G., 1996, MNRAS, 279, 49
Rauch M., 1998, ARA&A, 36, 267
Rauch M., Haehnelt M. G., Steinmetz M., 1997a, ApJ, 481, 601
Rauch M. et al., 1997, ApJ, 489, 7
Rees M. J., Ostriker J. P., 1977, MNRAS, 179, 541
Renzini A., 1997, ApJ, 488, 35
Schaye J., Rauch M., Sargent W. L. W., Kim T.-S., 2000a, ApJ, 541, L1
Schaye J., Theuns T., Rauch M., Efstathiou G., Sargent W. L. W., 2000b, MNRAS, 318, 817
Shaver P. A., Wall J. V., Kellermann K. I., Jackson C. A., Hawkins M. R. S., 1996, Nat, 384, 439
Steidel C. C., Giavalisco M., Pettini M., Dickinson M., Adelberger K. L., 1996, ApJ, 462, L17
Stengler-Larrea E. A., Webb J. K., 1993, in Chincarini G., Ionino A., Maccacaro T., Maccagni D., eds, ASP Conf. Ser. Vol. 51, Observational Cosmology. Astron. Soc. Pac., San Francisco, p. 591
Tegmark M., Silk J., Evrard A., 1993, ApJ, 417, 54
Theuns T., Leonard A., Efstathiou G., 1998a, MNRAS, 297, L49
Theuns T., Leonard A., Efstathiou G., Pearce F. R., Thomas P. A., 1998b, MNRAS, 301, 478
Thoul A. A., Weinberg D. H., 1996, ApJ, 465, 608
Wang B., 1995a, ApJ, 444, L17
Wang B., 1995b, ApJ, 444, 590
Webb J. K., 1987, PhD thesis, Univ. Cambridge
Wechsler R. H., Gross M. A. K., Primack J. R., Blumenthal G. R., Dekel A., 1998, ApJ, 506, 19
Weil M. L., Eke V. R., Efstathiou G., 1998, MNRAS, 300, 773
White S. D. M., Rees M. J., 1978, MNRAS, 183, 341
Wu K. K. S., Fabian A. C., Nulsen P. E. J., 2000a, MNRAS, 318, 889
Wu K. K. S., Fabian A. C., Nulsen P. E. J., 2000b, preprint (astro-ph/9910122)
Zhang Y., Anninos P., Norman M. L., 1995, ApJ, 453, L57

This paper has been typeset from a TEX/LATEX file prepared by the author.